chemosensors

MDPI

Article

MIP-Assisted 3-Hole POF Chip Faced with SPR-POF Sensor for Glyphosate Detection

Giancarla Alberti [1], Stefano Spina [2], Francesco Arcadio [2], Maria Pesavento [3], Letizia De Maria [4], Nunzio Cennamo [2], Luigi Zeni [2,*] and Daniele Merli [1,*]

[1] Department of Chemistry, University of Pavia, Via Taramelli 12, 27100 Pavia, Italy; giancarla.alberti@unipv.it
[2] Department of Engineering, University of Campania Luigi Vanvitelli, Via Roma 29, 81031 Aversa, Italy; stefano.spina@studenti.unicampania.it (S.S.); francesco.arcadio@unicampania.it (F.A.); nunzio.cennamo@unicampania.it (N.C.)
[3] Optosensing Srl, Via Carlo de Marco, 69/F, 80137 Napoli, Italy
[4] Ricerca sul Sistema Energetico (RSE) S.p.A, Via R. Rubattino 54, 20134 Milan, Italy; letizia.demaria@rse-web.it
* Correspondence: luigi.zeni@unicampania.it (L.Z.); daniele.merli@unipv.it (D.M.)

Abstract: The present study proposes the application of a recently developed optical–chemical sensor system to glyphosate detection. The device probes the refractive index variation in a chip based on a plastic optical fiber (POF) in which three orthogonal micro-holes were created and filled with an acrylic-based molecularly imprinted polymer (MIP). This sensitive chip, connected in series to a gold-coated SPR-POF platform, can modify the surface plasmon resonance (SPR) phenomena by exploiting the multimode characteristic of the POFs. Therefore, the gold film of the SPR-POF platform is not covered by the MIP layer, improving the sensor's performance because the interaction between the analyte (glyphosate) and the polymer recognition cavities occurs in the core and not in the cladding of the waveguide. Indeed, the sample solution is dropped on the MIP-based chip while a water drop is constantly maintained above the gold surface of the reference SPR-POF platform to excite the surface plasmons, modulated by the MIP interaction with the target analyte. The device is here for the first time applied for glyphosate sensing in water samples. The high sensitivity and selectivity are proven, and tests on real samples highlight the good performances of the developed sensors.

Keywords: glyphosate; molecularly imprinted polymer (MIP); surface plasmon resonance (SPR); plastic optical fiber (POF); environmental monitoring; optical–chemical sensors

Citation: Alberti, G.; Spina, S.; Arcadio, F.; Pesavento, M.; De Maria, L.; Cennamo, N.; Zeni, L.; Merli, D. MIP-Assisted 3-Hole POF Chip Faced with SPR-POF Sensor for Glyphosate Detection. *Chemosensors* **2023**, *11*, 414. https://doi.org/10.3390/chemosensors11070414

Academic Editor: Iole Venditti

Received: 25 June 2023
Revised: 10 July 2023
Accepted: 20 July 2023
Published: 22 July 2023

1. Introduction

Glyphosate (IUPAC name (N-phosphonomethyl)glycine) is a broad-spectrum and nonselective herbicide used worldwide [1,2]. It is usually distributed on the ground as aqueous solutions of about 0.03 M, but understanding and predicting its transport in soils is complicated [3–6]. Indeed, the challenges in detecting and proving glyphosate toxicity are probable due to its ability to chelate metal ions and interfere with the organic matter in the environment [3]. Moreover, it is considered harmful to humans and the environment and is suspected of being a carcinogen, associated with long-term effects for a prolonged exposition [3,7,8]. Although there is a connection between severe environmental and health problems, public health policies are absent, likely due to the difficulties in detecting glyphosate in the environment, which are additionally complicated by the invaluable health hazard and occupational safety [3].

This herbicide is the most widely and worldly employed in agriculture. However, it is difficult to be determined by classical analytical instrumental techniques, mainly because of its high polarity, high solubility in water and scarce solubility in organic solvents, low volatility, and strong metal complexation properties [3].

Up to now, several methods have been proposed for determining glyphosate in soil, agri-food products, beverages, and biological fluids; some also allow the detection of its primary metabolite, i.e., aminoethylphosphonic acid (AMPA) [9].

Colorimetric or fluorimetric methods are not viable since chromophore or fluorophore groups are absent in the glyphosate structure [3].

Chromatographic methods are the most common but require lengthy and time-consuming sample pretreatment and derivatization procedures; moreover, they need bulky, delicate, and expensive instruments [3,9–14]. Although glyphosate is non-electroactive, i.e., it cannot be measured at accessible potentials, several electrochemical sensors have been developed, but at present, none of them present an adequate level of sensitivity and reproducibility. Moreover, electrode surface modification or employing noble metal electrodes such as Pt or Ag is often required and is associated with laborious procedures, making these strategies inapplicable for real-time or in situ analysis [3,15–20].

Plastic optical fiber (POF)-based sensors, particularly those based on surface plasmon resonance (SPR), allow for the realization of small platforms integrable with compact optoelectronic instruments and suitable for determining different analytes with excellent sensitivity [21–23]. High selectivity for this kind of sensor is achieved by covering the plasmonic surface with a molecular recognition element that can be a bioreceptor or, more advantageously, a molecularly imprinted polymer (MIP) [23,24]. These kinds of devices are cheap and can be easily arranged in portable, in-field measurement devices.

At present, few studies reported the preparation of glyphosate-imprinted materials for sample preparation or sensors due to the low solubility of the analyte in porogenic solvents such as chloroform and the limited number of useful functional monomers [25–27]. Only one paper exploited the employment of SPR transduction faced with a molecularly imprinted electropolymerized polypyrrole film [28].

Recently, we proposed a new MIP-based SPR configuration [29,30] to overcome problems due to the MIP's film thickness and the deterioration of the sensitive gold surface of the SPR sensor. More specifically, in the conventional SPR approaches, a thick MIP layer can be used to reduce the bulk effect and the degradation of the SPR multilayer, but this thick MIP layer significantly reduces the sensitivity of the sensor system. Moreover, previous studies [31] demonstrated that the MIP refractive index increases as the amount of analyte entering the polymer recognition cavities increases, so the waveguide's effective refractive index also changes. In the sensor configuration reported in [29,30], when the analyte concentration increases, the MIP refractive index located in the core of POF increases too, and the resonance wavelength is blue-shifted (decreases) without changing the refractive index of the bulk solution in contact with the plasmonic surface [29,30].

The sensing device used in the present study comprises two POF-based chips in series. The first was prepared by creating three micro-holes in a POF and filling them with an acrylic-based molecularly imprinted polymer (MIP), and it is connected in series to a sensing gold-coated SPR-POF platform. The sample solution is dropped on the MIP-based chip while a water drop is constantly maintained above the gold surface of the SPR-POF platform to excite the surface plasmons, modulated by the MIP interaction with the target analyte that occurs in the core of the POF. The present approach modifies the SPR response of previously developed D-shaped POF plasmonic sensors [31–34] by changing how the light is launched into the sensor. To be precise, it takes advantage of the SPR phenomena to sense the variations of the light's propagation paths in the multimode POF resulting from the interaction of the target analyte with the MIP's recognition cavities.

Indeed, the gold surface of the SPR chip, not coated by the MIP or other receptor layers [32], is exploited to measure the variation of the core refractive index instead of detecting the refractive index variation of the receptor's dielectric layer directly over the sensing plasmonic surface as the SPR sensors previously proposed [31–34].

The excellent performance of the sensor was proven by detecting traces of 2-furaldehyde in water and milk samples [29,30].

The same innovative approach is exploited in the present study for sensing glyphosate in environmental waters. Analytical figures of merits of the presented method were highlighted and are in line with those of already existing analytical procedures in terms of sensitivity, linearity and detection limit (about 0.05 μg L^{-1} in the present case). Moreover, the method's performances were assessed by analyzing spiked natural water samples and comparing the results with those obtained by a validated HPLC-MS technique.

2. Materials and Methods

2.1. Reagents

Glyphosate (GLY, N-(Phosphonomethyl)glycine, Pestanal® analytical standard, (Sigma-Aldrich, St. Louis, MO, USA), acrylamide (AAM, suitable for electrophoresis, ≥99%), Ethylene Glycol Dimethylcrylate (EGDMA, 98%, d = 1.051 g/mL at 25 °C), 2,2′-azobisisobutyronitrile (AIBN), chloroform, dimethyl sulfoxide (DMSO), sodium hydroxide, acetic acid and ethanol, all ACS grade, were obtained from Merk Life Science S.r.l. (Milano, Italy) and used without further purification.

2.2. Prepolymeric Mixtures of MIP and NIP

The MIP prepolymeric mixture was prepared by adapting a previously proposed procedure [26]. The composition was adjusted to reduce the porogenic solvent, increasing the number of recognition holes. In total, 10 mg of GLY (template, 0.06 mmol), 0.25 g of AAM (functional monomer, 3.52 mmol) and 1 mL of EGDMA (cross-linker, 5.30 mmol) were mixed to obtain a polymer with a molar ratio of 1:60:90. To the mixture, 3 mL of 1:1 chloroform/DMSO solution was added to solubilize the template uniformly. The solution was sonicated and deaerated with a gentle flow of nitrogen for ten minutes; then, an excess of AIBN (40 mg) was added as a radical initiator. A similar prepolymeric mixture not containing GLY was prepared as the NIP (non-imprinted polymer).

2.3. Experimental Setup and Glyphosate Sensing

The sensing methodology utilized a MIP-modified POF chip that interacts with the analyte of interest connected to an SPR-POF sensor. A scheme of the experimental setup is shown in Figure 1 and includes a halogen lamp (for the MIP-based chip illumination), the MIP-functionalized chip, an SPR-POF platform and a spectrometer [29,30]. The employed halogen lamp has a wavelength emission ranging from 360 nm to 1700 nm (model HL2000-LL, Ocean Insight, Orlando, FL, USA), while the spectrum analyzer detection range is from 350 nm to 1000 nm (FLAME-S manufactured by Ocean Insight, Orlando, FL, USA). All the system components were connected by SMA connectors.

The MIP-modified POF platform consisted of a D-shaped POF chip in which three orthogonal micro-holes were performed and filled with the MIP (or NIP) prepolymeric mixture similar to [29,30]. The plastic optical fiber employed had a 1 mm diameter (980 μm PMMA core and 10 μm cladding). The POF was inserted in a resin block, and the D-shaped region (length: 1 cm) of the fiber was achieved through a polishing process using different grits of polishing papers (5 μm and 1 μm). The three micro-holes in the polished POF with a diameter of 600 μm and 2.5 mm apart from each other were created using a CNC micro-milling machine in an orthogonal orientation to the direction of the propagating light. The different distance between the micro-holes does not influence the sensor's sensitivity, as previously verified [29].

In a previous study [29], we compared the performance of the 3-hole POF platform with that of a single-hole POF chip. In terms of sensitivity at low concentrations, the 3-hole-based sensor performed better. The detection limit was lower with the one-hole system, but the linear concentration range was smaller than that with the three-hole. So, we decided to advance only with the development of the three-hole sensor.

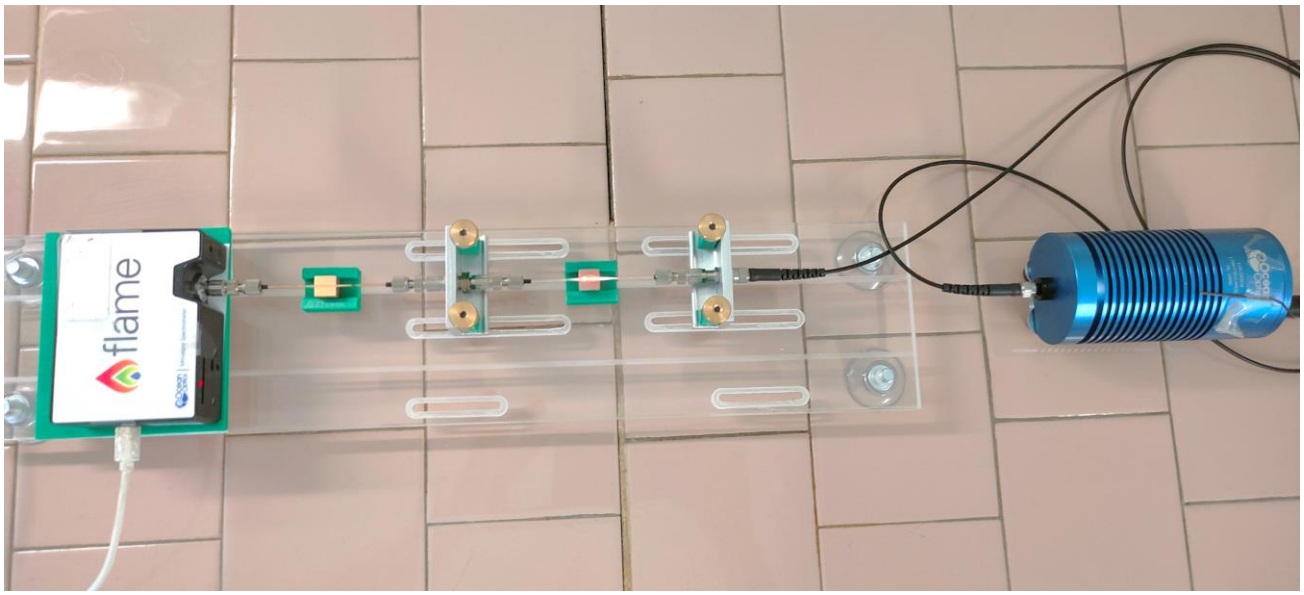

Figure 1. Experimental setup for glyphosate sensing by MIP-based 3-hole POF chip faced with SPR-POF sensor.

The chip's micro-holes must be filled with an adequate volume of the prepolymeric mixture, enough to completely fill each hole without overflowing; 8 µL of the prepolymeric solution was found to be the suitable volume. The polymerization was conducted thermally in a thermostated oven at 80 °C overnight. The template (GLY) was extracted from the MIP through 15 washing cycles with 0.1M NaOH. A final rinse with ultrapure water was necessary to eliminate the excess of NaOH; the chip was dried under a gentle flow of N_2 before the SPR measurements.

Figure 2a outlines the production steps of the MIP-based POF chemical chip, and Figure 2b shows the image of the 3-hole POF chip.

Like the previously described setup, the plasmonic probe consisted of a chip with a gold-photoresist multilayer (60 nm and 1 µm thick, respectively) on a planar surface of exposed-core POF (D-shaped POF region) introduced in a resin block [23]. In the present system, a constant amount of water on the gold layer surface was kept during the whole measurement period (refractive index 1.332). Since the water evaporation could induce variations if the thickness of the water layer decreases more than the field penetration, and consequently, in the water refractive index, the experiments were performed in a temperature-controlled room.

The dose–response curves were obtained by dropping 40 µL of a GLY aqueous standard solution at concentrations ranging from 100 ng L^{-1} (0.3 nM) to 1.5 mg L^{-1} (8.87 µM) onto the sensitive surface of the MIP-based chip and acquiring the spectra (with water over the SPR-POF platform) after a 10 min incubation period. These spectra are normalized on the reference spectrum acquired with air over the SPR-POF chip and 40 µL of ultrapure water on the MIP-based 3-hole POF platform (so that the SPR conditions are not satisfied).

The measured signal, $\Delta\lambda$, corresponded with the variation in the resonance wavelength occurring when the target analyte (GLY) interacted with the recognition cavities of the MIP's micro-holes, resulting in a local variation of the refractive index of the waveguide when compared to the response of a blank solution (ultrapure water). It has to be highlighted that the spectral resolution of the spectrometer employed here is 1.5 nm (calculated at the full width at half maximum, FWHM). However, the maximum value of the standard deviation of the resonance wavelength, experimentally determined by testing ten similar MIP-based 3-hole POF platforms repeating three times the tests for each chip, was about 0.15 nm.

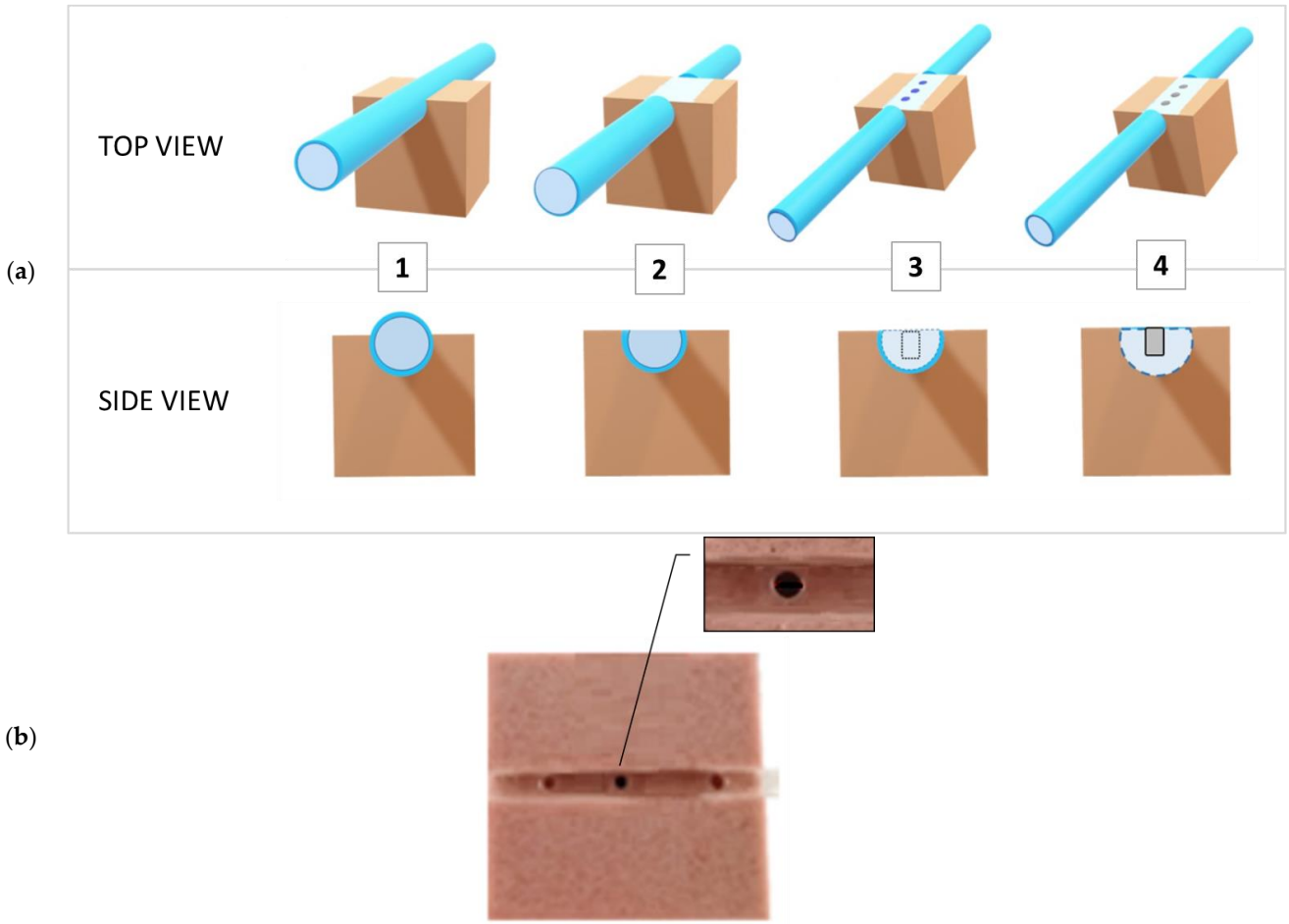

Figure 2. (**a**) Scheme of the preparation of the MIP-based 3-hole POF chip. (1) POF inserted in the resin block; (2) creation of the 1 cm D-shaped region of the POF; (3) preparation of three micro-holes with a diameter of 0.6 mm and 2.5 mm apart from each other; (4) micro-holes filled with the MIP. (**b**) picture (enlarged view 4×) of the 3-hole POF chip.

The calibration curves were obtained by correlating the Δλ values with the GLY concentration, *c*. From the linear part of the graph, the figures of merits of the method (detection limit, quantification limit, and sensitivity) were achieved. The entire dose–response dataset was modeled by the Hill equation for obtaining the affinity constant of the MIP's sites for the analyte [29–34].

3. Results

3.1. Dose–Response Curves: Figures of Merit of the Sensor

The figures of merit of the sensing method proposed here were evaluated by the dose–response curves; as an example, Figure 3 shows the SPR spectra obtained for different GLY aqueous solutions in the concentration range from 0.3 nM (100 ng L^{-1}) to 8.87 µM (1.5 mg L^{-1}).

The resonance wavelength shifted toward lower values (blue-shift) for increasing glyphosate concentration. This trend agrees with that previously observed [29], where the SPR wavelength decrease corresponded to a local increase in the POF core's refractive index.

Figure 4a shows a mean dose–response curve, Δλ (nm) vs. [GLY] (nM), obtained from independent calibrations performed with five MIP-based three-hole POF chips equally prepared. Figure 4b presents the same data with the abscissa in the logarithmic scale for more clear visualization of the trend.

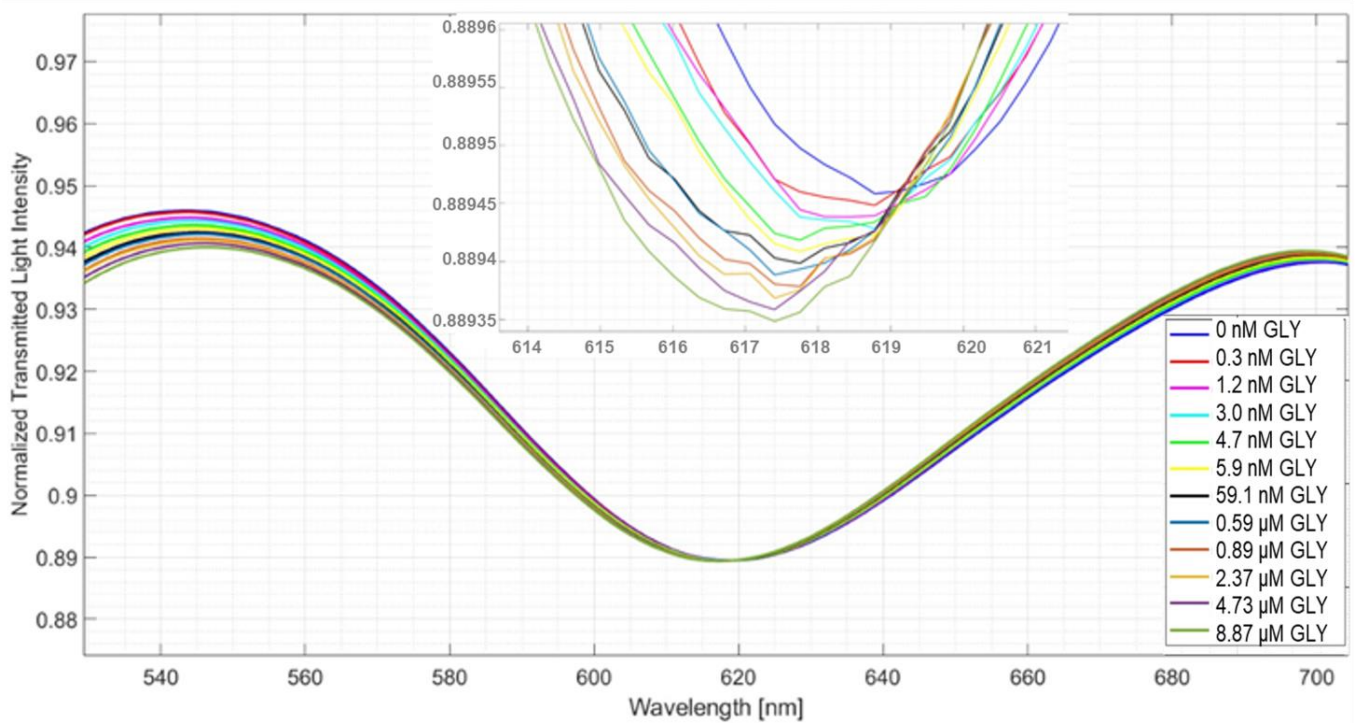

Figure 3. SPR spectra obtained for different glyphosate's aqueous solutions. In total, 40 µL of GLY solutions were dropped onto the MIP-based three-hole POF chip. The spectra were acquired with water over the SPR-POF platform after a 10 min incubation period. These spectra are normalized on the reference spectrum obtained with air over the SPR-POF chip and 40 µL of ultrapure water on the MIP-based three-hole POF platform.

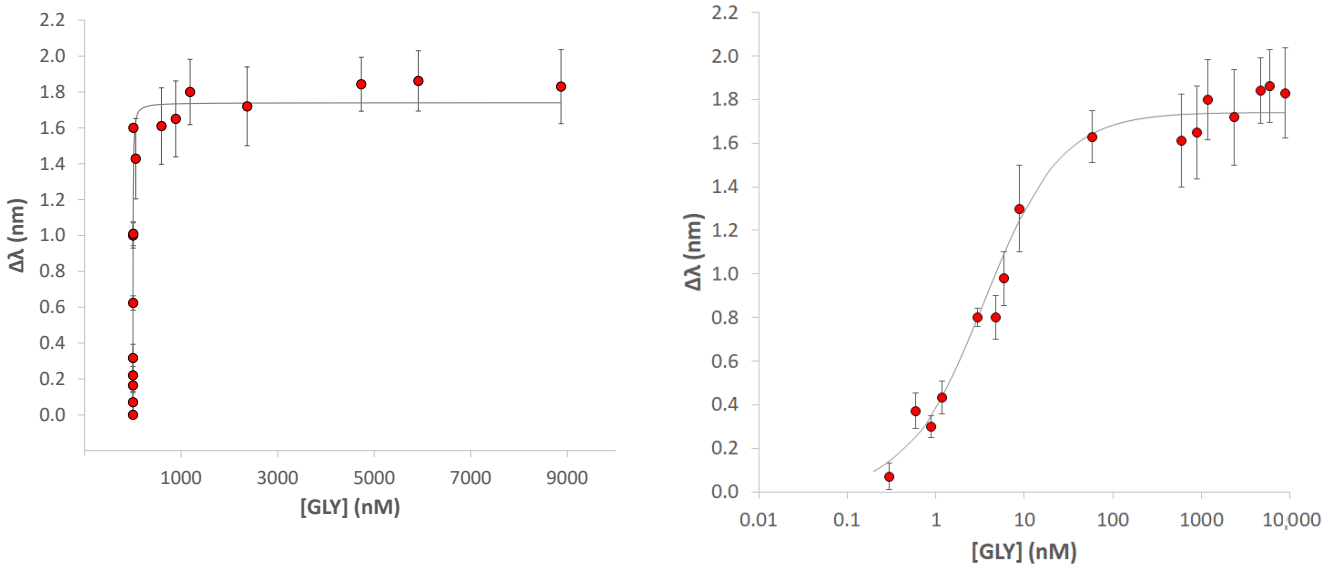

(**a**) (**b**)

Figure 4. (**a**) Dose–response curve Δλ (nm) vs. glyphosate concentration (nM) (**b**) the same graph with the abscissa in logarithmic scale. Experimental points are reported as the mean value of replicates obtained with five different chips. Error bars represent the standard deviation. The continuous curve represents the fitting by the Hill equation.

The dose–response curve is well-modeled by the Hill equation (Equation (1)), as previously reported for similar MIP-based sensors [29–34].

$$\Delta\lambda = |\lambda_c - \lambda_0| = \Delta\lambda_{max} \cdot \frac{c^n}{K^n + c^n} \quad (1)$$

where c is the glyphosate concentration, λ_c and λ_0 are, respectively, the resonance wavelength at the concentration c, and zero (blank), $\Delta\lambda_{max}$ is the maximum value of $\Delta\lambda_c$, i.e., the plateau of the curve correspondent to the analyte concentration for which saturation occurs due to the complete "filling" of the recognition cavities of the MIP. n was set at 1, assuming noncooperative and completely independent recognition sites in the MIP. K is the reciprocal of the affinity constant, K_{aff}, of the target analyte for the recognition cavities. $\Delta\lambda_{max}$ and K are the fitting parameters obtained by the OriginPro software [35].

The parameters of the Hill modeling to the experimental data reported in Figure 4 are summarized in Table 1.

Table 1. Parameters of the Hill equation (Equation (1)) for fitting the dose–response curve of Figure 4. The number in parenthesis is the standard deviation of the last digit.

$\Delta\lambda_{max}$ (nm)	K (M)	K_{aff} (M^{-1})	n	R^2
1.74 (4)	$3.5\ (6)\cdot10^{-9}$	$2.8\ (5)\cdot10^{8}$	1	0.907

The high value of the affinity constant is a measure of the high selectivity of the polymer.

The reproducibility, measured as replicates of the calibration of five different chips, is pretty good since the standard deviation is not higher than 0.25 nm for all the concentration levels.

The plateau of the curve was observed for a glyphosate concentration of about 50 nM so that the quantitative analysis can be performed only at lower concentrations. Indeed, the linear part of the dose–response curve (see Figure 5) can be used as a calibration plot from which the sensitivity at low concentrations and the detection and quantification limits (LOD and LOQ) can be determined.

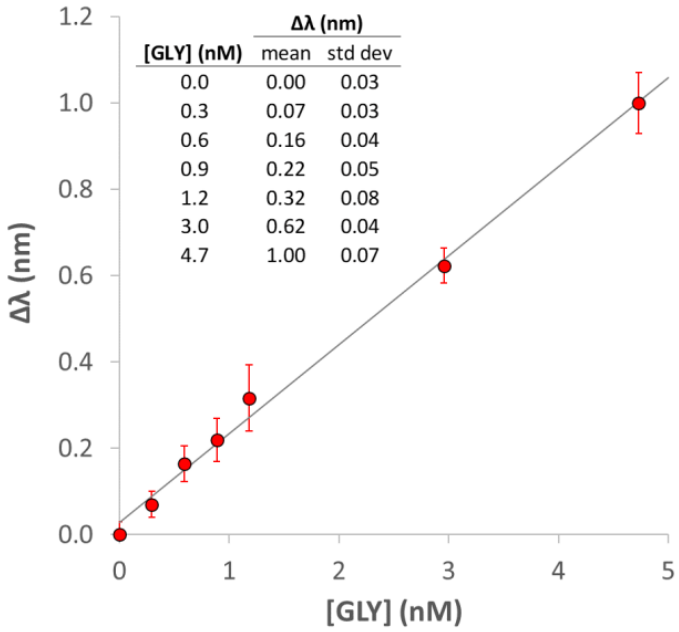

Figure 5. Linear part, at low concentrations of the dose–response curve Δλ (nm) vs. glyphosate concentration (nM) of Figure 4. Experimental points are reported as the mean value of replicates obtained with five different MIP-based three-hole POF chips, and the error bars represent the standard deviation.

Table 2 reports the method's figures of merit calculated from the parameters of the straight line interpolating the experimental data.

Table 2. Figures of merits evaluated from the linear regression of the data reported in Figure 5, i.e., dose–response curve at low concentrations. The number in parenthesis is the standard deviation of the last digit.

Slope (S, nm nM^{-1})	R^2	LOD [a] (nM)	LOQ (nM)	Linear Range (nM)
0.206 (6)	0.995	0.2	0.7	0.4–5

[a] LOD = $3.3 \cdot s_{y/x}/S$, $s_{y/x}$ is the standard deviation of y-residuals (i.e., the random errors in the y-direction); it is not significantly different from the standard deviation of multiple measurements of blank samples [36].

It is interesting to emphasize that the LOD and LOQ values obtained, converted into the unit of measurement used in regulatory rules, are, respectively, 0.04 μg L^{-1} and 0.11 μg L^{-1}; therefore, the proposed sensor is adequate to detect glyphosate at the concentrations levels compatible with the maximum residue limit (MRL) established by the Europe Community (MRL = 0.1 μg L^{-1}) for drinking water [37]. Moreover, the detection limit of the present sensor is comparable or lower to that of other analytical methods reported in the recent literature (see Table 3).

Table 3. Comparison of the detection limit of analytical methods and sensors for glyphosate detection in water samples.

Method/Sensor	Sample	LOD μg L^{-1}	Ref.
AgNPs-tailored SERS method [a]	distilled water	110	[38]
HPLC/fluorescence detector	seawater	0.6	[39]
LC-MS/MS	surface water	0.066	[40]
LC-MS/MS	environmental water	0.25	[41]
UHPLC-MS/MS	environmental water	0.025	[42]
reflectance spectroscopy immunosensor	drinking water	0.01	[43]
amperometric method/Au-SPC [b]	drinking water	270	[44]
dual-MIP-graphite SPE [c]	environmental water	0.7	[45]
MIPpy-based ESPR sensor [d]	distilled water	0.2	[28]
MIP-based three-hole POF chip/SPR-POF platform	drinking water	0.04	This work

[a] silver nanoparticles/surface-enhanced Raman spectroscopy; [b] amperometric method/gold working screen-printed electrode; [c] graphite screen-printed electrode modified with a dual-molecularly imprinted polymer coated on a mesoporous silica-platinum core; [d] electrochemical surface plasmon resonance sensor based on molecularly imprinted polypyrrole.

From Table 3, it can be observed that the lowest LOD is reached by the reflectance spectroscopy immunosensor [43]. Despite the LOD value being only four times lower than that obtained with the present sensor, developing an immunosensor requires many steps, and bioreceptors are unstable and delicate. Moreover, the sensor is not suitable for in situ analysis. Implementing simple and economical analytical systems, such as the proposed sensor, rather than those that can only boast performance at the research level, is often more valuable and practical.

Although it could be a stimulus and challenging to progress toward realizing a photonic integrated circuit, many technological and economic difficulties must be solved. Novel sensing approaches, such as those reported in [46–49], could be used to obtain high-performing integrated optical sensor chips. However, we prefer to develop sensors and methods with high selectivity and sensitivity of ready use, easy to realize and low cost.

3.2. Selectivity Tests and Real Samples Analysis

Selectivity tests were performed first by measuring glyphosate with NIP-based three-hole POF chips and then by analyzing samples containing another pesticide, bentazon,

as a possible interferent. Figure 6 shows the mean dose–response curve obtained from independent calibrations performed with three NIP-based three-hole POF chips equally prepared; the dose–response curve obtained with the five MIP-based three-hole POF chips was also reported for a direct comparison.

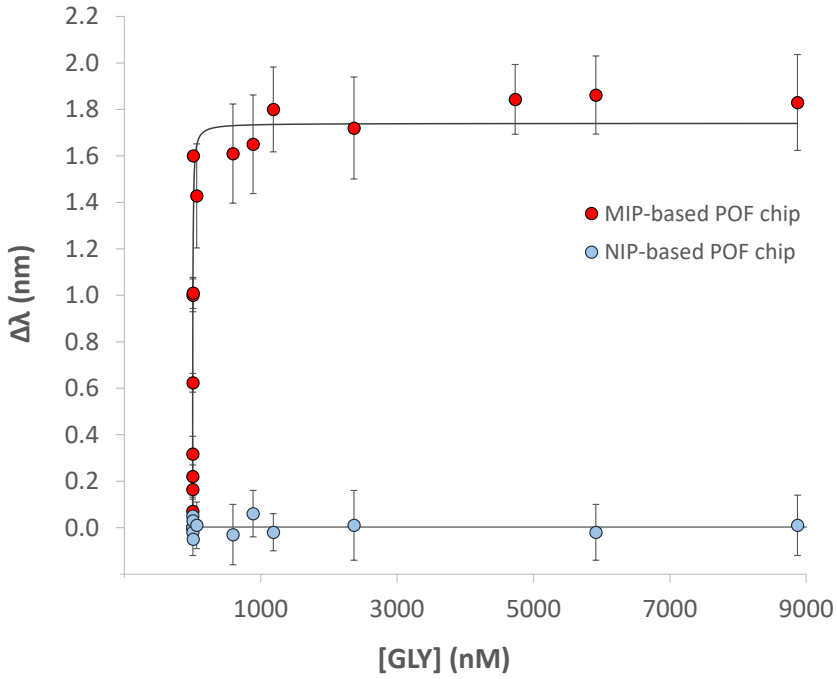

Figure 6. Dose–response curve Δλ (nm) vs. glyphosate concentration (nM). Experimental points for the NIP-based three-hole POF platforms (light blue points) are reported as the mean value of replicates obtained with three different chips. Error bars represent the standard deviation. The dose–response curve for the MIP-based three-hole POF chips (red points) is reported for comparison.

As can be seen from the graph of Figure 6, with the NIP-based three-hole POF chips, no significant shift of the resonance wavelength occurred for the standard solutions at different glyphosate concentrations, allowing the assertion that any non-specific interactions of the target analyte with the non-imprinted polymer are irrelevant to the SPR measurements.

Subsequently, sample solutions containing the herbicide bentazon (3-isopropyl-1H-2,1,3-benzothiadiazin-4(3H)-one 2,2-dioxide) were analyzed with the same MIP-based three-hole POF chip to prove the selectivity of the developed sensor. Figure 7 reports the SPR spectra obtained for two solutions containing bentazon, respectively, 0.4 µM and 1.7 µM (spectra red and fuchsia in Figure 7), and the spectrum of a blank solution (ultrapure water, spectrum blue in Figure 7) for comparison. No significant shift in the resonance wavelength was observed despite the high (µM range) analyte concentration. Conversely, the blue shift occurred only in the presence of glyphosate, as evident from the spectra obtained for glyphosate solutions, respectively, 3.0 nM and 60 nM (light blue and green spectra in Figure 7).

To verify the applicability of the developed sensing system to the analysis of environmental waters, two samples of drinking water (sampled from the tap of the lab) were fortified with two different glyphosate concentrations: sample (a) with GLY 0.89 nM, i.e., 0.15 µg L^{-1} and sample (b) with GLY 1.18 nM, i.e., 0.2 µg L^{-1}. The standard addition method was applied for glyphosate quantification, and the graphs are shown in Figure 8. The recovery percentage is reported in Table 4, with the concentration obtained from the analysis of the same samples by LC-MS as a reference method. For these tests, two different MIP-based three-hole POF chips were employed.

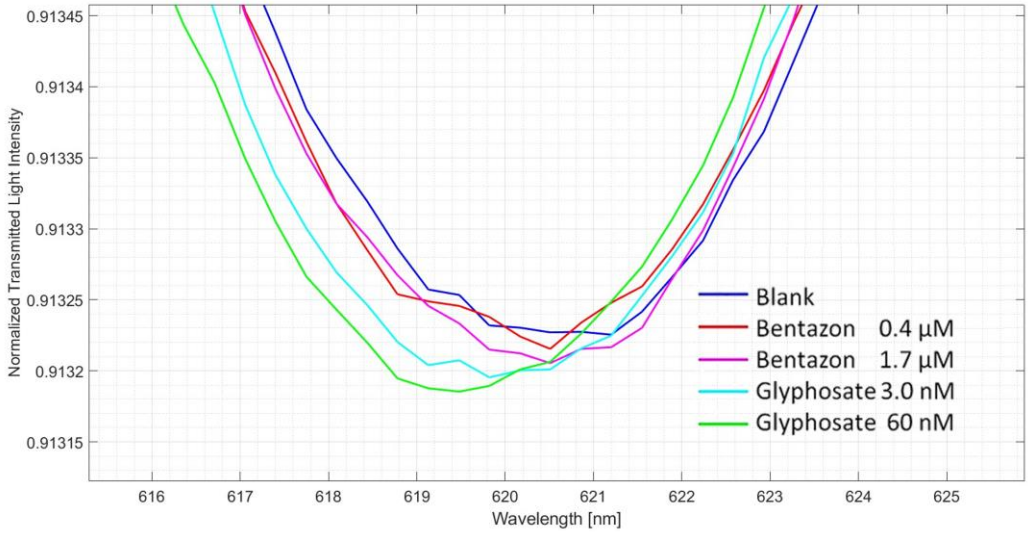

Figure 7. Normalized SPR spectra obtained with the MIP-based POF chip for aqueous solutions of Bentazon and Glyphosate.

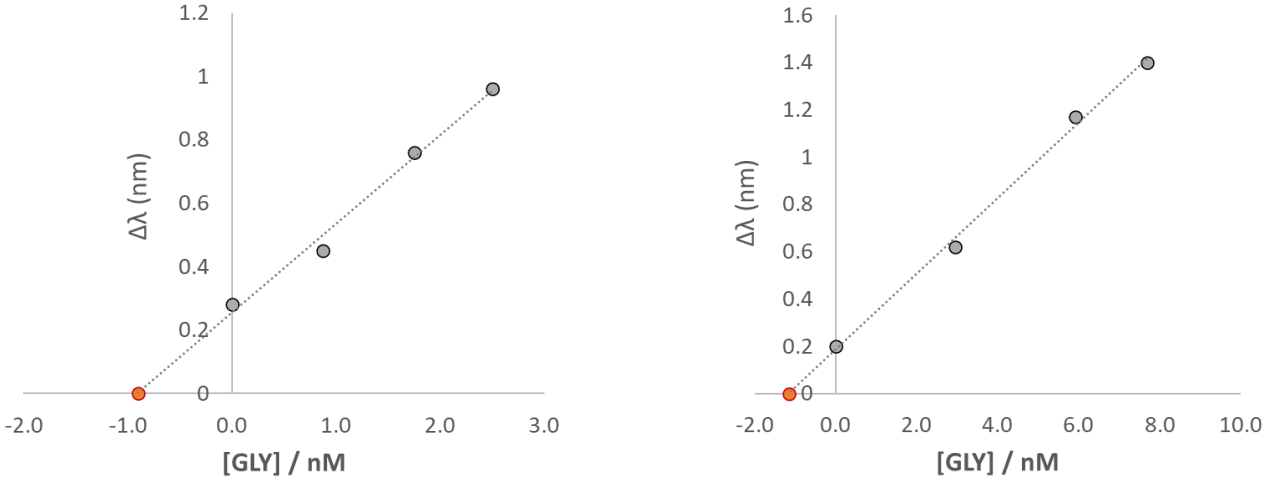

Figure 8. Standard addition method's graph (**a**) for the tap water sample spiked with GLY 0.89 nM; (**b**) for the tap water sample spiked with GLY 1.18 nM. The concentration in the test sample is the x-intercept of the plot (orange point in the graph), and its value is computed by the ratio of the y-intercept and the slope of the regression line.

Table 4. Determination of glyphosate in fortified drinking water samples by the MIP-based POF chip/SPR-POF platform. The number in parenthesis is the standard deviation on the last digit.

Sample	$[GLY]_{added}$ (nM)	$[GLY]_{found}$ (nM)	Recovery%	Error%	$[GLY]_{LC-MS}$ (nM)
(a)	0.89	0.90 (8)	102	+1.8	0.85 (5)
(b)	1.18	1.16 (9)	98	−2.0	1.20 (3)

The results obtained with the MIP-based POF chip and SPR-POF platform are in good agreement with those achieved with the chromatographic method; moreover, the high recovery % and the low error % make the method promising for environmental analysis.

4. Conclusions

The present study demonstrated the excellent performances of a MIP-based three-hole POF chip combined with an SPR-POF platform for glyphosate detection at very low concentrations (nM level). The device examines the refractive index variation in the chip realized by drilling three micro-holes in a POF, orthogonally to the fiber axis, and filled with molecularly imprinted polymer (MIP), selective for the target analyte. The MIP-based chip is connected in series to a sensing SPR-POF platform so that the MIP-glyphosate interaction modifies the surface plasmon resonance phenomena without changing the medium in contact with the SPR surface.

The good selectivity and the high sensitivity at low analyte concentrations make the sensor promising for glyphosate detection at trace concentrations in environmental samples; moreover, the detection limit achieved is lower than the maximum residue limit (MRL) established by the EU (0.1 $\mu g\ L^{-1}$) for drinking waters, making the method adequate for glyphosate sensing, also in non-contaminated waters.

The easy realization, the relatively low cost of the instrumentation, and the reduced volume of sample required for the analysis are further advantages for future in-field applications (being the instrument portable) for the continuous monitoring of the contamination of this herbicide in the environment.

Author Contributions: Conceptualization, N.C., L.Z., M.P. and G.A.; methodology, N.C., M.P., L.Z. and F.A.; software, S.S. and F.A.; formal analysis, G.A.; investigation, S.S.; data curation, G.A. and D.M.; writing—original draft preparation, G.A.; writing—review and editing, D.M., N.C., F.A. and L.D.M.; supervision, L.Z. All authors have read and agreed to the published version of the manuscript.

Funding: This research received no external funding.

Institutional Review Board Statement: Not applicable.

Informed Consent Statement: Not applicable.

Data Availability Statement: All data used are presented in the paper.

Acknowledgments: The authors acknowledge the BETTER project founded by POR FESR Campania (2014–2020) and the support from the Ministero dell'Università e della Ricerca (MUR) and the University of Pavia through the program "Dipartimenti di Eccellenza 2023–2027".

Conflicts of Interest: The authors declare no conflict of interest.

References

1. Woodburn, A.T. Glyphosate: Production, pricing and use worldwide. *Pest. Manag. Sci.* **2000**, *56*, 309–312. [CrossRef]
2. Castle, L.A.; Siehl, D.L.; Gorton, R.; Patten, P.A.; Chen, Y.H.; Bertain, S.; Cho, H.-J.; Duck, N.; Wong, J.; Liu, D.; et al. Discovery and directed evolution of a glyphosate tolerance gene. *Science* **2004**, *304*, 1151–1154. [CrossRef]
3. Valle, A.L.; Mello, F.C.C.; Alves-Balvedi, R.P.; Rodrigues, L.P.; Goulart, L.R. Glyphosate detection: Methods, needs and challenges. *Environ. Chem. Lett.* **2019**, *17*, 291–317. [CrossRef]
4. Candela, L.; Caballero, J.; Ronen, D. Glyphosate transport through weathered granite soils under irrigated and non-irrigated conditions—Barcelona, Spain. *Sci. Total. Environ.* **2010**, *408*, 2509–2516. [CrossRef] [PubMed]
5. Laitinen, P.; Rämö, S.; Nikunen, U.; Jauhiainen, L.; Siimes, K.; Turtola, E. Glyphosate and phosphorus leaching and residues in boreal sandy soil. *Plant Soil* **2009**, *323*, 267–283. [CrossRef]
6. Tuesca, D.; Puricelli, E. Effect of tillage systems and herbicide treatments on weed abundance and diversity in a glyphosate resistant crop rotation. *Crop Prot.* **2007**, *26*, 1765–1770. [CrossRef]
7. Benachour, N.; Séralini, G.-E. Glyphosate formulations induce apoptosis and necrosis in human umbilical, embryonic, and placental cells. *Chem. Res. Toxicol.* **2009**, *22*, 97–105. [CrossRef]
8. Tsui, M.T.K.; Chu, L.M. Environmental fate and non-target impact of glyphosate-based herbicide (Roundup®) in a subtropical wetland. *Chemosphere* **2008**, *71*, 439–446. [CrossRef]
9. Zambrano-Intriago, L.A.; Amorim, C.G.; Rodríguez-Díaz, J.M.; Araújo, A.N.; Montenegro, M.C. Challenges in the design of electrochemical sensor for glyphosate-based on new materials and biological recognition. *Sci. Total Environ.* **2021**, *793*, 148496. [CrossRef] [PubMed]
10. Sun, L.; Kong, D.; Gu, W.; Guo, X.; Tao, W.; Shan, Z.; Wang, Y.; Wang, N. Determination of glyphosate in soil/sludge by high performance liquid chromatography. *J. Chromatogr. A* **2017**, *1502*, 8–13. [CrossRef]

11. Koskinen, W.C.; Marek, L.J.; Hall, K.E. Analysis of glyphosate and aminomethylphosphonic acid in water, plant materials and soil. *Pest. Manag. Sci.* **2016**, *72*, 423–432. [CrossRef] [PubMed]
12. Zhang, W.; Feng, Y.; Ma, L.; An, J.; Zhang, H.; Cao, M.; Zhu, H.; Kang, W.; Lian, K. A method for determining glyphosate and its metabolite aminomethyl phosphonic acid by gas chromatography-flame photometric detection. *J. Chromatogr. A* **2018**, *1589*, 116–121. [CrossRef] [PubMed]
13. Liao, Y.; Berthion, J.M.; Colet, I.; Merlo, M.; Nougadère, A.; Hu, R. Validation and application of analytical method for glyphosate and glufosinate in foods by liquid chromatography–tandem mass spectrometry. *J. Chromatogr. A* **2018**, *1549*, 31–38. [CrossRef]
14. Royer, A.; Beguin, S.; Tabet, J.C.; Hulot, S.; Reding, M.A.; Communal, P.Y. Determination of glyphosate and aminomethylphosphonic acid residues in water by gas chromatography with tandem mass spectrometry after exchange ion resin purification and derivatization. Application on vegetable matrixes. *Anal. Chem.* **2000**, *72*, 3826–3832. [CrossRef] [PubMed]
15. Oliveira, G.C.; Moccelinia, S.K.; Castilhoa, M.; Terezoa, A.J.; Possavatzb, J.; Magalhãesb, M.R.L.; Doresb, E.F.G.C. Biosensor based on atemoya peroxidase immobilised on modified nanoclay for glyphosate biomonitoring. *Talanta* **2012**, *98*, 130–136. [CrossRef]
16. Khenifi, A.; Derriche, Z.; Forano, C.; Prevot, V.; Mousty, C.; Scavetta, E.; Ballarin, B.; Guadagnini, L.; Tonelli, D. Glyphosate and glufosinate detection at electrogenerated NiAl-LDH thin films. *Anal. Chim. Acta* **2009**, *654*, 97–102. [CrossRef]
17. Méndez, M.A.; Suárez, M.F.; Cortés, M.T.; Sarria, V.M. Electrochemical properties and electro-aggregation of silvercarbonate sol on polycrystalline platinum electroda and its alactrocatalytic activity towards glyphosate oxidation. *Electrochem. Commun* **2007**, *9*, 2585–2590. [CrossRef]
18. Bataller, R.; Campos, I.; Laguarda-Miro, N.; Alcañiz, M.; Soto, J.; Martínez-Máñez, R.; Gil, L.; García-Breijo, E.; Ibáñez-Civera, J. Glyphosate Detection by Means of a Voltammetric Electronic Tongue and Discrimination of Potential Interferents. *Sensors* **2012**, *12*, 17553–17568. [CrossRef] [PubMed]
19. Ding, S.; Lyu, Z.; Li, S.; Ruan, X.; Fei, M.; Zhou, Y.; Niu, X.; Zhu, W.; Du, D.; Lin, Y. Molecularly imprinted polypyrrole nanotubes based electrochemical sensor for glyphosate detection. *Biosens. Bioelectron.* **2021**, *191*, 113434. [CrossRef]
20. Jiang, R.; Pang, Y.H.; Yang, Q.Y.; Wan, C.Q.; Shen, X.F. Copper porphyrin metal-organic framework modified carbon paper for electrochemical sensing of glyphosate. *Sens. Actuators B Chem.* **2022**, *358*, 131492. [CrossRef]
21. Leung, A.; Shankar, P.M.; Mutharasan, R. A review of fiber-optic biosensors. *Sens Actuators B Chem.* **2007**, *125*, 688–703. [CrossRef]
22. Gupta, B.D.; Verma, R.K. Surface plasmon resonance-based fiber optic sensors: Principle, probe designs, and some applications. *J. Sens.* **2009**, *2009*, 979761. [CrossRef]
23. Cennamo, N.; Pesavento, M.; Zeni, L. A review on simple and highly sensitive plastic optical fiber probes for bio-chemical sensing. *Sens. Actuators B Chem.* **2021**, *331*, 129393. [CrossRef]
24. Gupta, B.D.; Shrivastav, A.M.; Usha, S.P. Surface Plasmon Resonance-Based Fiber Optic Sensors Utilizing Molecular Imprinting. *Sensors* **2016**, *16*, 1381. [CrossRef]
25. Zarejousheghani, M.; Jaafar, A.; Wollmerstaedt, H.; Rahimi, P.; Borsdorf, H.; Zimmermann, S.; Joseph, Y. Rational Design of Molecularly Imprinted Polymers Using Quaternary Ammonium Cations for Glyphosate Detection. *Sensors* **2021**, *21*, 296. [CrossRef] [PubMed]
26. da Mata, K.; Corazza, M.Z.; de Oliveira, F.M.; de Toffoli, A.L.; Teixeira Tarley, C.R.; Moreira, A.B. Synthesis and characterization of cross-linked molecularly imprinted polyacrylamide for the extraction/preconcentration of glyphosate and aminomethylphosphonic acid from water samples. *React. Funct. Polym.* **2014**, *83*, 76–83. [CrossRef]
27. Gomez-Caballero, A.; Diaz-Diaz, G.; Bengoetxea, O.; Quintela, A.; Unceta, N.; Goicolea, M.A.; Barrio, R.J. Water compatible stir-bar devices imprinted with underivatised glyphosate for selective sample clean-up. *J. Chromatogr. A* **2016**, *1451*, 23–32. [CrossRef]
28. Balciunas, D.; Plausinaitis, D.; Ratautaite, V.; Ramanaviciene, A.; Ramanavicius, A. Towards electrochemical surface plasmon resonance sensor based on the molecularly imprinted polypyrrole for glyphosate sensing. *Talanta* **2022**, *241*, 123252. [CrossRef]
29. Cennamo, N.; Arcadio, F.; Zeni, L.; Alberti, G.; Pesavento, M. Optical-Chemical Sensors based on plasmonic phenomena modulated via micro-holes in Plastic Optical Fibers filled by Molecularly Imprinted Polymers. *Sens. Actuators B Chem.* **2022**, *372*, 132672. [CrossRef]
30. Alberti, G.; Arcadio, F.; Pesavento, M.; Marzano, C.; Zeni, L.; Zeid, N.A.; Cennamo, N. Detection of 2-Furaldehyde in Milk by MIP-Based POF Chips Combined with an SPR-POF Sensor. *Sensors* **2022**, *22*, 8289. [CrossRef]
31. Cennamo, N.; De Maria, L.; D'Agostino, G.; Zeni, L.; Pesavento, M. Monitoring of Low Levels of Furfural in Power Transformer Oil with a Sensor System Based on a POF-MIP Platform. *Sensors* **2015**, *15*, 8499–8511. [CrossRef] [PubMed]
32. Pesavento, M.; Profumo, A.; Merli, D.; Cucca, L.; Zeni, L.; Cennamo, N. An Optical Fiber Chemical Sensor for the Detection of Copper(II) in Drinking Water. *Sensors* **2019**, *19*, 5246. [CrossRef] [PubMed]
33. Pesavento, M.; Zeni, L.; De Maria, L.; Alberti, G.; Cennamo, N. SPR-Optical Fiber-Molecularly Imprinted Polymer Sensor for the Detection of Furfural in Wine. *Biosensors* **2021**, *11*, 72. [CrossRef]
34. Cennamo, N.; D'Agostino, G.; Pesavento, M.; Zeni, L. High selectivity and sensitivity sensor based on MIP and SPR in tapered plastic optical fibers for the detection of L-nicotine. *Sens. Actuators B Chem.* **2014**, *191*, 529–536. [CrossRef]
35. *OriginPro*; Version 2015; OriginLab Corporation: Northampton, MA, USA, 2015.
36. Miller, J.N.; Miller, J.C. Calibration methods in instrumental analysis: Regression and correlation. In *Statistics and Chemometrics for Analytical Chemistry*, 6th ed.; Pearson Education Limited: Harlow Essex, UK, 2010; pp. 124–126.

37. EFSA (European Food Safety Authority). Conclusion on the peer review of the pesticide risk assessment of the active substance glyphosate. *EFSA J.* **2015**, *13*, 4302.
38. Costa, L.D.C.S.; Schiefer, E.M.; Fabris, J.L.; Muller, M. Detection of Glyphosate in Water with Photonic-Tailored Silver Nanoparticles. In Proceedings of the 2022 SBFoton International Optics and Photonics Conference (SBFoton IOPC), Recife, Brazil, 13–15 October 2022.
39. Wang, S.; Liu, B.; Yuan, D.; Ma, J. A simple method for the determination of glyphosate and aminomethylphosphonic acid in seawater matrix with high performance liquid chromatography and fluorescence detection. *Talanta* **2016**, *161*, 700–706. [CrossRef]
40. Poiger, T.; Buerge, I.J.; Bächli, A.; Müller, M.D.; Balmer, M.E. Occurrence of the herbicide glyphosate and its metabolite AMPA in surface waters in Switzerland determined with on-line solid phase extraction LC-MS/MS. *Environ. Sci. Pollut. Res. Int.* **2017**, *24*, 1588–1596. [CrossRef]
41. Okada, E.; Coggan, T.; Anumol, T.; Clarke, B.; Allinson, G. A simple and rapid direct injection method for the determination of glyphosate and AMPA in environmental water samples. *Anal. Bioanal. Chem.* **2019**, *411*, 715–724. [CrossRef]
42. Campanale, C.; Triozzi, M.; Massarelli, C.; Uricchio, V.F. Development of a UHPLC-MS/MS method to enhance the detection of Glyphosate, AMPA and Glufosinate at sub-microgram/L levels in water samples. *J. Chromatogr. A* **2022**, *1672*, 463028. [CrossRef]
43. Stavra, E.; Petrou, P.S.; Koukouvinos, G.; Economou, A.; Goustouridis, D.; Misiakos, K.; Raptis, I.; Kakabakos, S.E. Fast, sensitive and selective determination of herbicide glyphosate in water samples with a White Light Reflectance Spectroscopy immunosensor. *Talanta* **2020**, *214*, 120854. [CrossRef]
44. Noori, J.S.; Dimaki, M.; Mortensen, J.; Svendsen, W.E. Detection of Glyphosate in Drinking Water: A Fast and Direct Detection Method without Sample Pretreatment. *Sensors* **2018**, *18*, 2961. [CrossRef] [PubMed]
45. Thimoonnee, S.; Somnet, K.; Ngaosri, P.; Chairam, S.; Karuwan, C.; Kamsong, W.; Tuantranont, A.; Amatatongchai, M. Fast, sensitive and selective simultaneous determination of paraquat and glyphosate herbicides in water samples using a compact electrochemical sensor. *Anal. Methods* **2022**, *14*, 820–833. [CrossRef] [PubMed]
46. Kish, F.; Lal, V.; Evans, P.; Corzine, S.W.; Ziari, M.; Butrie, T.; Reffle, M.; Tsai, H.-S.; Dentai, A.; Pleumeekers, J.; et al. System-on-chip photonic integrated circuits. *IEEE J. Sel. Top. Quantum Electron.* **2017**, *24*, 1–20. [CrossRef]
47. Milanizadeh, M.; Ahmadi, S.; Petrini, M.; Aguiar, D.; Mazzanti, R.; Zanetto, F.; Guglielmi, E.; Sampietro, M.; Morichetti, F.; Melloni, A. Control and calibration recipes for photonic integrated circuits. *IEEE J. Sel. Top. Quantum Electron.* **2020**, *26*, 1–10. [CrossRef]
48. Barreda, I.; Otaduy, D.; Martín-Rodríguez, R.; Merino, S.; Fernández-Luna, J.L.; González, F.; Moreno, F. Electromagnetic behavior of dielectric objects on metallic periodically nanostructured substrates. *Opt. Express* **2018**, *26*, 11222. [CrossRef] [PubMed]
49. Díaz-Escobar, E.; Bauer, T.; Pinilla-Cienfuegos, E.; Barreda, Á.I.; Griol, A.; Kuipers, L.; Martínez, A. Radiationless anapole states in on-chip photonics. *Light Sci. Appl.* **2021**, *10*, 204. [CrossRef]